Neurotoxicology 73 (2019) 142–149

Contents lists available at ScienceDirect

Neurotoxicology

journal homepage: www.elsevier.com/locate/neuro

Full Length Article

Involvement of mitogen-activated protein kinase pathways in ferrous iron-induced aquaporin-4 expression in cultured astrocytes

Zhihong Zhong[a,1], Yuhao Sun[a,1], Baofeng Wang[a], Qingfang Sun[a], Guoyuan Yang[b], Liuguan Bian[a,*]

[a] Department of Neurosurgery, Ruijin Hospital, Shanghai Jiao Tong University School of Medicine, Shanghai 200025, China
[b] Neuroscience and Neuroengineering Research Center, Med-X Research Institute, Shanghai Jiao Tong University, Shanghai 200030, China

ARTICLE INFO

Keywords:
Aquaporin-4
Ferrous iron
Astrocyte
Oxidative stress
Mitogen-activated protein kinases

ABSTRACT

Iron is an essential element for multiple metabolic reactions, but excessive iron accumulation in the brain can lead to astrocyte swelling and death and cause cerebral edema. Aquaporin-4 (AQP4) is the important water channel expressed in the astrocytes, and maintains the water homeostasis of the brain. Previous study has shown that iron deposition could increase AQP4 expression, however, the mechanism of AQP4 expression upregulation after iron overload is still unclear. In this study, we investigated the effect of ferrous iron overload on AQP4 expression in cultured mouse astrocytes. Primary cultures of astrocytes were exposed to ferrous iron, and the expression of AQP4 as well as the swelling of astrocyte were determined. AQP4 expression was inhibited by small interfering RNA (siRNA). The role of oxidative stress and mitogen-activated protein kinases (MAPKs) signaling pathway in ferrous iron-induced AQP4 expression upregulation were further studied. Ferrous iron exposure induced astrocyte death as well as cell swelling, and increased AQP4 expression. AQP4 gene silencing after siRNA transfection attenuated ferrous iron-induced astrocyte death. After treatment with antioxidants, the increased AQP4 expression was diminished. MAPKs were activated after ferrous iron treatment, and inhibitors of ERK and p38-MAPK relieved AQP4 expression upregulation as well as astrocyte death. These results suggest that ferrous iron has distinctive toxic effects on cultured astrocytes and induces AQP4 expression upregulation. MAPKs activation may play important roles in ferrous iron-induced astrocyte death through upregulation of AQP4 expression.

1. Introduction

Iron is an essential component for various metabolic reactions, including DNA synthesis, enzymatic reactions, and electron transport in the respiratory chain (Ward et al., 2014; Ximenes-da-Silva, 2016). However, excess iron accumulation in the brain can harm biological systems, and lead to neurological disorders such as Parkinson's disease and Alzheimer's disease (Belaidi and Bush, 2016; Jiang et al., 2009). In addition, overload of iron released from the hematoma after intracerebral hemorrhage (ICH) has been shown to contribute to brain injury (Qing et al., 2009). Previous studies have demonstrated that iron overload could independently induce neuronal death, resulting in injury of astrocyte and cerebral edema (Qing et al., 2009; Ward et al., 2014; Wu et al., 2011).

Aquaporin-4 (AQP4), the principal water channel in the brain, is mainly expressed in the plasma membranes of astrocytes. Previous studies have reported that AQP4 is associated with neurodegenerative processes in mouse models of Parkinson's disease and Alzheimer's disease (Chi et al., 2011; Liu et al., 2012). Moreover, due to its important role in brain water and ion homeostasis, AQP4 has been implicated in cerebral edema in various pathological conditions, including ischemia, trauma, and tumors (Higashida et al., 2011a, b; Nico and Ribatti, 2011; Shenaq et al., 2012). Numerous studies have also demonstrated that AQP4 contributes to the formation of cerebral edema following ICH (Qing et al., 2009; Wu et al., 2010). Therefore, regulation of AQP4 expression in astrocytes may provide a potential therapeutic option for neurological disorders.

It has been reported that some metals, such as manganese and mercury, can affect AQP4 expression in astrocytes (Rao et al., 2010; Yamamoto et al., 2012). Previous study has demonstrated that iron deposition, accompanied with increased AQP4 expression, was observed in the perihematomal brain of rat (Qing et al., 2009). Also, our

* Corresponding author at: Department of Neurosurgery, Ruijin Hospital, Shanghai Jiao Tong University, School of Medicine, 197, Rui Jin Er Road, Shanghai 200025, China.
E-mail address: blg11118@rjh.com.cn (L. Bian).
[1] Equal contributor.

https://doi.org/10.1016/j.neuro.2019.03.006
Received 28 November 2018; Received in revised form 27 February 2019; Accepted 21 March 2019
Available online 23 March 2019
0161-813X/

previous study has shown that iron overload can induce AQP4 upregulation in cultured astrocytes (Wang et al., 2015). However, the mechanism of upregulation of AQP4 expression after iron overload is still unclear.

Mitogen-activated protein kinases (MAPKs), a group of serine/threonine specific protein kinases, are involved in various cellular roles, such as proliferation, cell survival, and apoptosis. Previous studies have reported that MAPKs can be activated by diverse extracellular factors, including oxidative stress (OS), osmolality changes, and proinflammatory cytokines (Sigala et al., 2011; Song et al., 2016; Yang et al., 2013b). Further evidences showed that the activation of MAPKs can lead to AQP4 overexpression in different conditions (Song et al., 2016; Tang et al., 2013; Yang et al., 2013b). However, it is unknown whether MAPKs activation is the mechanism of AQP4 upregulation in astrocytes under iron overload.

In the present study, we examined AQP4 expression in cultured astrocytes after treatment with Fe^{2+}, as well as the role of MAPKs in AQP4 expression.

2. Materials and methods

2.1. Astrocyte culture

Primary cultures of cortical astrocytes were prepared from cerebral cortices of C57BL/6 mice born within 48 h as described previously (Wang et al., 2015). Briefly, the cerebral cortices were separated from meninges and basal ganglia, trypsinized at 37 °C, dissociated in Dulbecco's modified Eagle's medium supplemented with 10% fetal bovine serum and penicillin/streptomycin, and then seeded onto poly-D-lysine coated plates. The medium was replaced after 24 h, and then changed every 2–3 days. After grown to 80% confluency, the cells were subsequently trypsinized and subcultured. More than 95% of the cells were astrocytes, as determined by immunostaining with anti-glial fibrillary acidic protein (GFAP) antibody.

2.2. Ferrous iron exposure and agent treatment

Cultured astrocytes were randomly divided into control group and Fe^{2+}-exposure group. In Fe^{2+}-exposure group, pilot experiments were carried out to obtain an optimal concentration of Fe^{2+}. Cultured cells were exposed to ferrous chloride ($FeCl_2$) (Sinopharm Chemical Reagent Co, Ltd, China) in concentrations of 10, 25, 50 and 100 μM. Results showed that 25 μM was the optimal concentration, which was described in Section 3. In the MAPK inhibitors (U0126, SB203580, and SP600125) or antioxidants (Vitamin E and L-NAME) studies, reagents were added to cells in the specified concentration for 1 h prior to treatment with Fe^{2+}.

The used MAPK inhibitors and antioxidants were as following: SB203580 (p38 inhibitor) (Santa Cruz Biotechnology, USA), U0126 (ERK1/2 inhibitor) (Santa Cruz Biotechnology, USA), SP600125 (JNK inhibitor) (Santa Cruz Biotechnology, USA), Vitamin E (Sigma-Aldrich, USA), and L-NAME (Sigma-Aldrich, USA).

2.3. Cell viability assay

Cell viability was assessed by 2-(2-methoxy-4-nitrophenyl)-3-(4-nitrophenyl)-5-(2,4-disulfophenyl)-2H-tetrazolium, monosodium salt (WST-8) with a Cell Counting kit-8 (CCK-8) assay (Dojindo, Japan), as described previously (Dai et al., 2013). In brief, cells were cultured in a 96-well plate, and 100 μl of cell suspension was incubated with 10 μl of WST-8 solution at 37 °C for 4 h. The absorbance of the samples at 450 nm wavelength was measured by a microplate reader (BioTek, USA).

2.4. Estimation of cell volume

Astrocyte volume was analyzed following the method of Yang et al. (Yang et al., 2013b). Briefly, the 10-Hz confocal x–y images of the cultured astrocyte in control group or Fe^{2+}-exposure group were acquired and converted to a binary format using the Image J software (V1.40). The comparative z-stack was traced and confirmed by the appropriation of the z-plane with the largest surface area, as well as cross-referencing fluorescence intensity from other areas of the selected image. Then the cell volume was calculated by the particle analysis software in Image J. At least 10 independent cells in each group were analyzed from at least three separate experiments.

2.5. Immunocytochemistry

Astrocytes plated on coverslips were fixed in 4% paraformaldehyde for 10 min and washed with 0.1 mol/L PBS. The cells were permeabilized with 0.3% Triton for 10 min, blocked in 10% bovine serum albumin for 30 min, and then incubated overnight at 4 °C with primary antibodies: rabbit anti-AQP4 (1:200, Santa Cruz Biotechnology, USA), and mouse anti-GFAP (1:200, Millipore, USA). On the following day, the cells were washed and incubated with secondary antibodies: Alexa Fluor 488 donkey anti-rabbit IgG (1:500, Invitrogen, USA) and Alexa Fluor 594 donkey anti-mouse IgG (1:500, Invitrogen, USA) for 1 h. The cells were washed again and incubated with DAPI (1:2,000, Sigma, USA) for 10 min. After washing with PBS, the cells were mounted on slides. Then confocal microscopic images were acquired using a Leica confocal laser-scanning microscope (Leica, Wetzlar, Hesse, Germany).

2.6. Relative quantitative real-time PCR analysis

Total RNA was isolated from the cultured astrocytes using Trizol reagent (Invitrogen, USA). Reverse transcription was performed using a PrimeScript RT reagent kit (TaKaRa Bio Inc., China). The oligonucleotide primers used to amplify target genes were as follows: AQP4, 5′-CTGGAGCCAGCATGAATCCAG-3′ (forward) and 5′-TTCTTCTCTTCT CCACGGTCA-3′ (reverse); GAPDH, 5′- AGGTCGGTGTGAACGGAT TTG-3′ (forward) and 5′- TGTAGACCATGTAGTTGAGGTCA-3′ (reverse). All primers were obtained from Invitrogen Corp (Shanghai). After 40 cycles, the relative levels of mRNA expression were quantified with SDS software (Applied Biosystems, Carlsbad, CA).

2.7. Western blot analysis

Proteins were extracted from the cultured astrocytes after the treatments, and protein concentrations were determined by a bicinchoninic acid protein assay kit (Pierce Biotechnology, USA). Equal amounts of proteins (50 μg) were loaded onto a 12% polyacrylamide gel for electrophoresis, and then electro-transferred onto polyvinylidenedifluoride membrane. Blots were blocked with 5% non-fat milk, and incubated at 4 °C overnight with primary antibodies against AQP4 (1:200, Santa Cruz Biotechnology, USA), α-tubulin (1:1000, Cell Signaling Technology, USA), ERK (1:1000, Cell Signaling Technology, USA), phospho-ERK (1:1000, Cell Signaling Technology, USA), JNK (1:1000, Cell Signaling Technology, USA), phospho-JNK (1:1000, Cell Signaling Technology, USA), p38 (1:1000, Cell Signaling Technology, USA), phospho-p38 (1:1000, Cell Signaling Technology, USA). After washing, the membranes were incubated with Goat anti-rabbit HRP (1:2000, HangZhouHuaAn Biotechnology Co, China) for 1 h at room temperature. Protein signals were then detected by ECL chemiluminescence system (Pierce Biotechnology, USA). Densitometric analysis of bands was determined by Image J software (V1.40).

2.8. Transfection of AQP4 small interfering ribonucleic acid

Cells were transfected with AQP4 small-interfering RNA (siRNA) or

nontargeting control siRNA (Guangzhou Ribobio Co, Ltd, China) using Lipofectamine 2000 (Invitrogen, USA), according to the manufacturer's instructions. Briefly, Lipofectamine 2000 was diluted 1:50 (v/v) in OPTIMEM low serum medium (Invitrogen, USA) and incubated for 5 min at room temperature. Then AQP4 siRNA and nontargeting control siRNA were diluted in OPTIMEM medium, added separately into Lipofectamine 2000, and incubated for 20 min at room temperature. The mixture containing siRNA and Lipofectamine 2000 was then added to cultured cells, and the transfection was taken place over 48 h.

2.9. Statistical analysis

All data were expressed as the mean ± SE. For analysis between two groups of the cell volume and cell viability, the expression of each molecule, the Student's *t*-test was performed. A p-value of < 0.05 was considered statistically significant. Calculations were done with the SPSS version 20 software and the GraphPad Prism software package 4.0.

3. Results

3.1. Effect of Fe^{2+} on cell viability and cell volume of cultured astrocytes

The viability of astrocytes incubated with Fe^{2+} at different concentrations (10, 25, 50 and 100 μM) and different time points (1, 3, 6, 12, and 24 h) was shown in Fig. 1A. After Fe^{2+} treatment, there was no significant change in cell viability at 1 h ($p > 0.05$), while decreased cell viability of astrocytes was observed at 3 h ($p < 0.05$), which further declined gradually in 6–24 h ($p < 0.05$). And the viability of astrocytes incubated with Fe^{2+} at 10, 25, 50, and 100 μM for 24 h showed a dose-dependent manner of Fe^{2+} toxicity on astrocytes.

Cell volume of the cultured astrocytes was measured to determine the effect of Fe^{2+} on astrocyte swelling (Fig. 1B). Compared with the control group, cell volume increased significantly after Fe^{2+} (10, 25 and 50 μM) treatment as early as 3 h ($p < 0.05$), reaching a peak at about 12–24 h ($p < 0.05$). Inversely, 100 μM of Fe^{2+} reduced cell volume of the cultured astrocytes significantly in a time-dependent manner ($p < 0.05$).

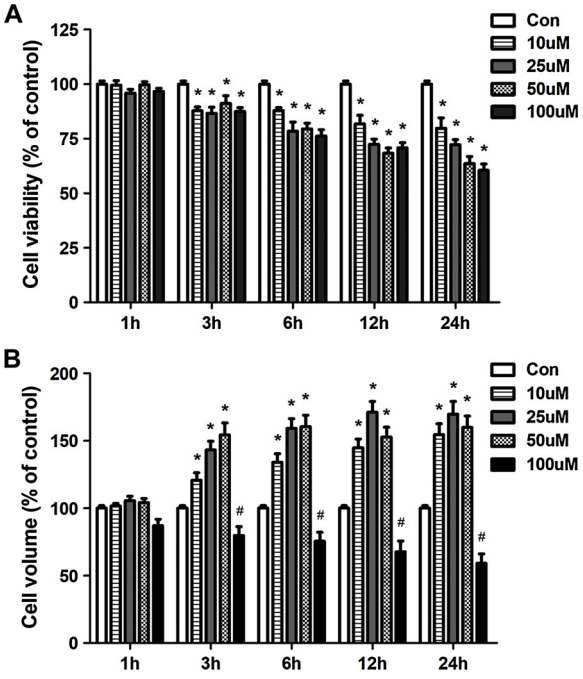

Fig. 1. Fe^{2+}-induced astrocyte death and cell swelling. Cultured astrocytes were exposed to different concentrations of Fe^{2+} (10, 25, 50 and 100 μM) for certain periods (1, 3, 6, 12, and 24 h). (A) Fe^{2+} had distinctive toxic effects on cultured astrocytes in a time- and dose-dependent manner. n = 5 for each group. Values are mean ± SE. *$p < 0.05$ vs. control group. (B) Cell volume increased time-dependently after treatment with 10, 25, and 50 μM of Fe^{2+}. Inversely, after incubation with 100 μM of Fe^{2+}, cell volume decreased in a time-dependent manner. n = 10 for each group. Values are mean ± SE. *$p < 0.05$ vs. control group. #$P < 0.05$ vs. control group.

3.2. Effect of Fe^{2+} on AQP4 expression in cultured astrocytes

To determine the influence of Fe^{2+} on AQP4 expression in cultured astrocytes, cells were treated with 10, 25, 50 and 100 μM of Fe^{2+} at the indicated times (1, 3, 6, 12, and 24 h) before total RNA isolation for RT-PCR or protein harvesting for western blot. As shown by the results of RT-PCR and immunoblot analysis, with the increase of Fe^{2+} concentration (10, 25, 50, and 100 μM), the mRNA levels of AQP4 as well as AQP4 protein levels were upregulated, reaching a peak at 25 μM ($p < 0.01$) (Fig. 2B and D). Compared with controls, Fe^{2+} induced AQP4 mRNA levels upregulation as early as 1 h with peaking at 3 h ($p < 0.01$), while AQP4 protein expression increased at 3 h, reaching a peak at 6 h ($p < 0.01$) (Fig. 2A and C). In addition, immunofluorescence staining also showed that the protein levels of AQP4 were significantly increased in cultured astrocytes at 6 h after Fe^{2+} (25 μM) treatment (Fig. 2E).

Combining with the results of cell viability, cell volume and AQP4 expression of cultured astrocytes after Fe^{2+} treatment, we chose the Fe^{2+} concentration of 25 μM as the optimal concentration for the following studies.

3.3. Effect of Fe^{2+} on MAPKs activation in cultured astrocytes

To investigate whether MAPKs are activated in cultured astrocytes under Fe^{2+} overload, the phosphorylated and the total amounts of each of the three MAPKs were measured by western blot at the indicated times (1, 3, 6, 12, and 24 h). After Fe^{2+} (25 μM) treatment, the three MAPKs were significantly activated in cultured astrocytes ($p < 0.05$) (Fig. 3). Fe^{2+} upregulated the phosphorylation of p38-MAPK and ERK as early as 3 h ($p < 0.05$), while the phosphorylation of JNK was activated at 6 h ($p < 0.05$). The p-ERK activation peaked at 12 h after Fe^{2+} exposure ($p < 0.01$). The increase of p-p38 MAPK, p-ERK and p-JNK persisted for at least 24 h.

3.4. AQP4 gene silencing attenuates Fe^{2+}-induced astrocyte death

Transfection of AQP4 siRNA (100 nM) into cultured astrocytes significantly reduced the AQP4 expression ($p < 0.05$), while control siRNA had no such effect on AQP4 protein expression ($p > 0.05$) (Fig. 4A). Significant cell death was observed in cultured astrocytes transfected with control siRNA after Fe^{2+} treatment, whereas astrocytes transfected with AQP4 siRNA showed a marked reduction in Fe^{2+}-induced cell death ($p < 0.05$) (Fig. 4B).

3.5. Antioxidants diminish Fe^{2+}-induced AQP4 upregulation and astrocyte death

We examined the effect of antioxidants on AQP4 protein expression in cultured astrocytes after Fe^{2+} treatment. The results showed that Vitamin E (250 μM) and L-NAME (250 μM) could significantly diminish Fe^{2+}-induced AQP4 protein upregulation as well as astrocyte death ($p < 0.05$) (Fig. 5A and B). Treatment with antioxidants alone in cultured astrocytes (without Fe^{2+} treatment) showed no significant change in AQP4 protein expression ($p > 0.05$) (Fig. 5C).

3.6. MAPK kinase inhibitors reduce Fe^{2+}-induced AQP4 upregulation and astrocyte death

To investigate the possible involvement of the three MAPK

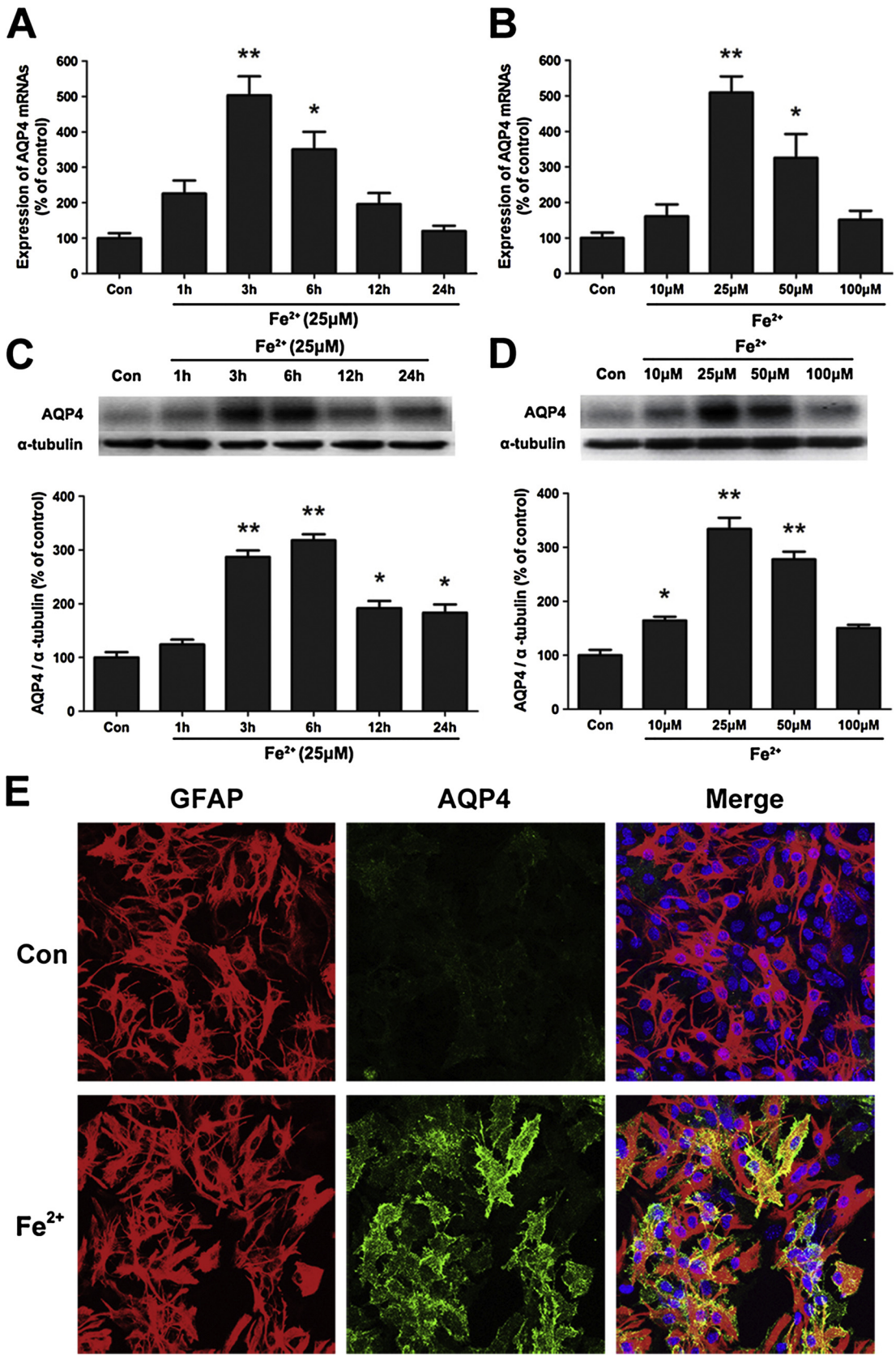

Fig. 2. Effect of Fe^{2+} on the expression of AQP4 in cultured astrocytes. (A) Time course of AQP4 mRNA expression after exposure to Fe^{2+} (25 μM). (B) AQP4 mRNA expression significantly increased after treatment with 25 and 50 μM of Fe^{2+} for 3 h. (C) Time course of AQP4 protein expression after exposure to Fe^{2+} (25 μM). (D) AQP4 protein expression significantly increased after treatment with 10, 25 and 50 μM of Fe^{2+} for 6 h. (E) Immunofluorescence staining showed significant increased AQP4 expression in cultured astrocytes after treatment with Fe^{2+}. n = 3 for each group. Values are mean ± SE. *p < 0.05 vs. control group. **P < 0.01 vs. control group.

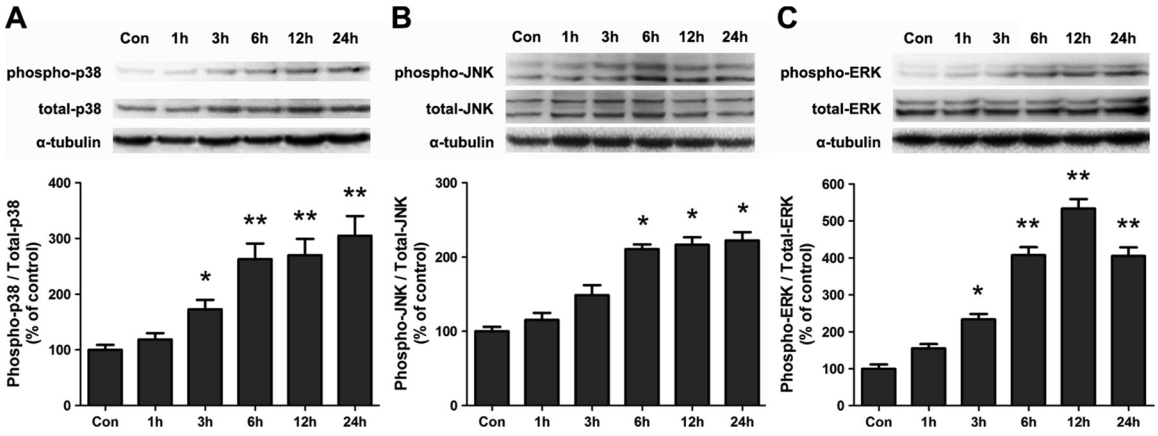

Fig. 3. Effect of Fe^{2+} (25 μM) on MAPKs activation in cultured astrocytes. (A and B) Fe^{2+} upregulated the phosphorylation of p38 and JNK in a time-dependent manner. (C) After treatment with Fe^{2+}, the phosphorylation of ERK was activated at 3 h, reaching a peak at 12 h. n = 3 for each group. Values are mean ± SE. *p < 0.05 vs. control group. **P < 0.01 vs. control group.

pathways in the increased AQP4 expression after Fe^{2+} overload, the cultured astrocytes were pretreated with the p38-MAPK inhibitor SB203580 (5 μM), the JNK inhibitor SP600125 (5 μM), and the ERK inhibitor U0126 (5 μM), respectively. As shown by the results of immunoblot analysis and CCK-8 (Fig. 6A and B), Fe^{2+}-induced AQP4 expression upregulation and astrocyte death were significantly inhibited by U0126 and SB203580 ($p < 0.05$). In contrast, SP600125 (1–10 μM) had no significant effect on AQP4 protein upregulation induced by Fe^{2+} ($p > 0.05$) (Fig. 6C). All three MAPK inhibitors did not influence the basal expression of AQP4 ($p > 0.05$) (Fig. 6D).

4. Discussion

In the present study, our findings showed that Fe^{2+} had distinctive toxic effects on cultured astrocytes in a time- and dose-dependent manner. And Fe^{2+} treatment resulted in significant upregulation of AQP4 expression in cultured astrocytes. Further experiments showed that the mechanism of AQP4 upregulation in cultured astrocytes after Fe^{2+} treatment might involve OS and MAPK signaling pathway activation.

AQP4 is the main water channel expressed in astrocytes in the CNS (Jung et al., 1994). Some metal ions such as lead, mercury, and manganese can affect AQP4 expression in the CNS and change water permeability in brain cells, resulting in neuronal damage (Gunnarson et al., 2005; Rao et al., 2010; Yamamoto et al., 2012; Yukutake et al., 2008). Ferrous iron is a product of hemoglobin degradation and plays a crucial role in cerebral edema and brain damage (Hua et al., 2007, 2006; Huang et al., 2002). In ICH rat models, Qing et al. have demonstrated that iron content increases in the perihematomal zone after ICH onset and peaks at day 7, and AQP4 expression in the perihematomal brain is also upregulated following ICH and peaks at day 3 (Qing et al., 2009). Further application of the iron chelator deferoxamine could reduce iron deposition and AQP4 level in the perihematomal area, indicating a correlation between iron content and AQP4 expression (Qing et al., 2009). And our previous study showed that iron overload could increase AQP4 expression in astrocytes *in vitro* (Wang et al., 2015). In the present study, we further demonstrated that ferrous iron could upregulate AQP4 expression in astrocytes in a time-dependent manner with a peak at 3–6 h. We also found that AQP4 expression increased in a dose-dependent manner at lower concentrations, whereas it began to decline at higher concentrations. We speculated that increased astrocytic death at higher concentrations resulted in reduced AQP4 expression reversely. In addition, we observed a marked reduction of Fe^{2+}-induced cell death in cultured astrocytes transfected with AQP4 siRNA, suggesting an important role of AQP4 in astrocyte death caused by ferrous iron. The mechanism of AQP4 upregulation resulting in astrocyte death after Fe^{2+} treatment is unclear. Combined the results of CCK-8 with cell volume measurement, we presume that it may be related to increased water transportation and the consequent cytotoxic edema caused by AQP4 upregulation. Chu et al. reported that AQP4 deletion increased apoptosis in AQP4 knockout mouse ICH model, indicating the protective effect of AQP4 other than promotive effect on

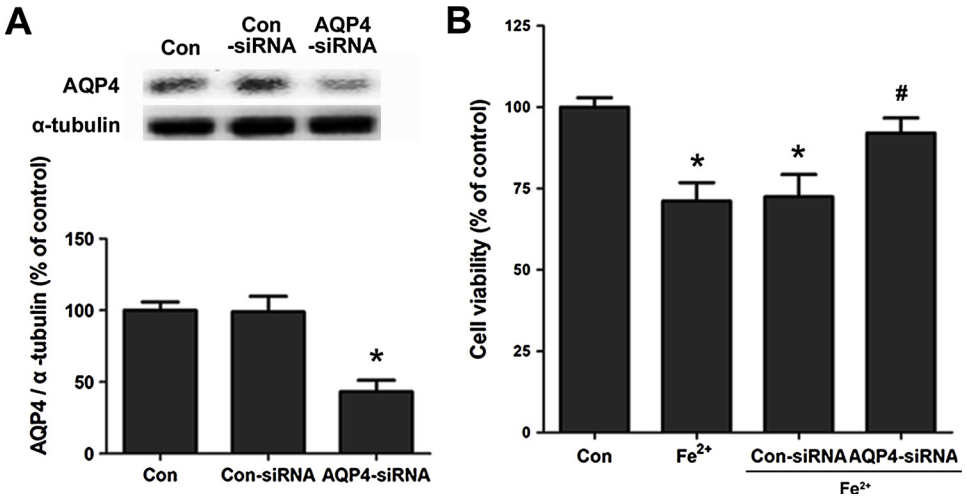

Fig. 4. Effect of AQP4 gene silencing on Fe^{2+}-induced astrocyte death. (A) AQP4 expression decreased significantly after transfection with AQP4 siRNA (100 nM). n = 3 for each group. (B) Fe^{2+}-induced astrocyte death was significantly attenuated by AQP4 siRNA transfection (100 nM). n = 5 for each group. Values are mean ± SE. *p < 0.05 vs. control group.

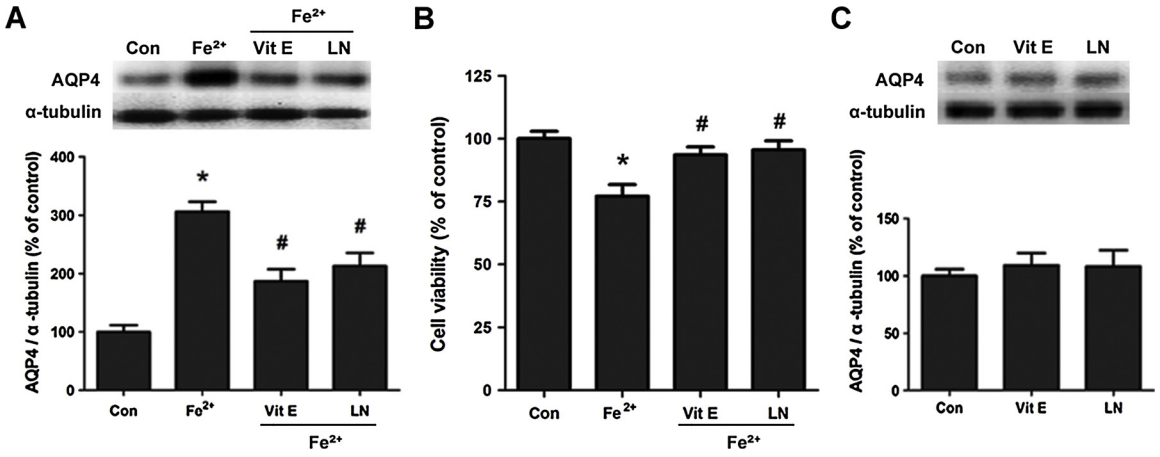

Fig. 5. Effect of antioxidants on Fe^{2+}-induced AQP4 upregulation and astrocyte death. (A and C) Both vitamin E (250 μM) and L-NAME (250 μM) significantly diminished AQP4 expression induced by Fe^{2+}, while treatment with antioxidants alone showed no significant influence on AQP4 protein expression. n = 3 for each group. Values are mean ± SE. *p < 0.05 vs. control group. #P < 0.05 vs. Fe^{2+}-exposure group. (B) Antioxidants significantly attenuated Fe^{2+}-induced astrocyte death. n = 5 for each group. Values are mean ± SE. *p < 0.05 vs. control group. #P < 0.05 vs. Fe^{2+}-exposure group.

apoptosis (Chu et al., 2014). Thus we speculate that the mechanism of AQP4 upregulation resulting in astrocyte death under Fe^{2+} overload may involve in necrosis or other style of cell death rather than apoptosis. It need to be investigated in further studies.

However, Lee et al. reported that AQP4 expression in primary cultured rat astrocytes was not affected by high extracellular iron concentrations (Lee et al., 2008). But in their study the agent added to the cultured astrocytes was ferric iron (Fe^{3+}). Unlike Fe^{3+}, Fe^{2+} can generate reactive oxygen species and induce OS via the Fenton's reaction, and then cause tissue damage (Crichton et al., 2002). In the present study, we observed a blockade of Fe^{2+}-induced AQP4 expression increase in astrocytes after treatment with antioxidants (Vit E and L-NAME), indicating that Fe^{2+} might upregulate the expression of AQP4 by a process involving generation of reactive oxygen species and induction of OS.

Astrocytes play a pivotal role in brain homeostasis and metabolism, including ion and water transportation, chemical signal transmission, and OS defense (Liu et al., 2017). Elevated harmful stimuli can disrupt the homeostasis and exhaust the neuroprotective mechanisms of astrocytes. Under iron overload condition, excessive iron can be transported into astrocytes and then cause cytotoxic effect. The mechanism of iron accumulation in astrocytes under iron overload involves distinct routes. One route mediates the uptake of transferrin-bound iron with transferrin receptors (Qian et al., 1999). A second route involves a transferrin-independent mechanism in which the uptake of ferrous iron depends on divalent metal transporter 1 and ascorbate (Lane et al., 2010). Also, there is a third route in which the uptake of ferric iron mediated by a mechanism independent of transferrin receptors or ascorbate/divalent metal transporter 1, and conditions with limitations in ascorbate may switch iron uptake to this route (Skjorringe et al., 2015). We speculate that transferrin/transferrin receptors route may be the possible mechanism involved under Fe^{2+} overload in our study in which ferric iron and ascorbate were limited. After the increased uptake of Fe^{2+} into the astrocytes, Fe^{2+} further causes injury cascade.

MAPKs are known as important stress-responsive signaling pathways commonly activated by OS (Kyriakis and Avruch, 1996), mainly including extracellular signal-regulated kinase (ERK), c-Jun N-terminal kinase (JNK), and p38 MAPK signaling. Previous studies have shown that MAPKs are involved in regulating several AQPs. AQP1 expression is upregulated around blood vessels due to activation of MAPK/JNK signaling in subarachnoid hemorrhage (Yatsushige et al., 2007), while MAPK/ERK signaling induces AQP1 expression in cultured astrocytes following injury (McCoy and Sontheimer, 2010). After hyperosmotic solution exposure, inhibition of MAPK/ERK signaling pathway can attenuate the expression of AQP3, AQP5, and AQP8 (Yang et al., 2013b), whereas the p38 inhibitor can inhibit the expression of AQP9 in cultured astrocytes (Arima et al., 2003; Yang et al., 2013b). AQP4 expression was reported to be mitigated by inhibition of MAPKs pathways overactivation under various conditions, such as hyperosmotic solution exposure, hypoxia-induced brain edema and ischemic stroke (Arima et al., 2003; Wang et al., 2018a, b; Yang et al., 2013b; Yuen et al., 2017). In this study, we detected an increase in phosphorylation of ERK, JNK, and p38 as well as AQP4 expression after treatment with Fe^{2+}, as indicated by Western blot. Pretreating the astrocytes with ERK and p38-MAPK inhibitors could suppress Fe^{2+}-induced AQP4 expression upregulation and astrocyte death, suggesting that AQP4 expression in cultured astrocytes under iron overload condition can be regulated by MAPK/ERK and p38 MAPK pathways. Furthermore, it indicates that MAPKs may contribute to Fe^{2+}-induced astrocyte death by a process involving increases in AQP4 expression.

In addition, our study showed that only ERK and p38-MAPK inhibitors reduced Fe^{2+}-induced AQP4 expression and astrocyte death, although Fe^{2+} activates all three MAPKs pathways. The reason that JNK inhibitor is unable to block AQP4 upregulation and astrocyte death induced by Fe^{2+} is unclear. This phenomenon is similar to that described in a previous study in which other than the JNK inhibitor, the ERK and p38-MAPK inhibitors could attenuate manganese-induced AQP4 expression and astrocyte swelling (Rao et al., 2010). Rao et al. speculated that MAPKs may differentially regulate downstream pathways that variably influence AQP4 expression (Rao et al., 2010).

MAPKs pathways are related to the activation of NF-κB and subsequent regulation of cellular genes under multiple stimuli (Adachi et al., 2012). Evidence has shown that ERK signaling can activate NF-κB (Cassarino et al., 2000). And phosphorylated p38-MAPK has been demonstrated to activate IκB kinase and then lead to NF-κB activation (de Alvaro et al., 2004). JNK is thought to play an opposite role versus ERK and p38-MAPK to NF-κB (Shi et al., 2016). This may partially explain the phenomenon that only the ERK and p38-MAPK inhibitors can reduce Fe^{2+}-induced AQP4 expression and astrocyte death. In our previous study, we have found that NF-κB/p65 subunit in the cytoplasm and nucleus of cultured astrocytes were elevated after treatment with Fe^{2+} (Wang et al., 2015). By inhibiting the activation of NF-κB, AQP4 expression would be reduced, indicating that NF-κB plays an important role in regulating AQP4 expression (Wang et al., 2015). However, whether ERK and p38-MAPK signaling contribute directly as an upstream regulator or indirectly to stimulate the transcriptional activity of NF-κB is further to be determined.

NF-κB is a pivotal transcription factor that is involved in the

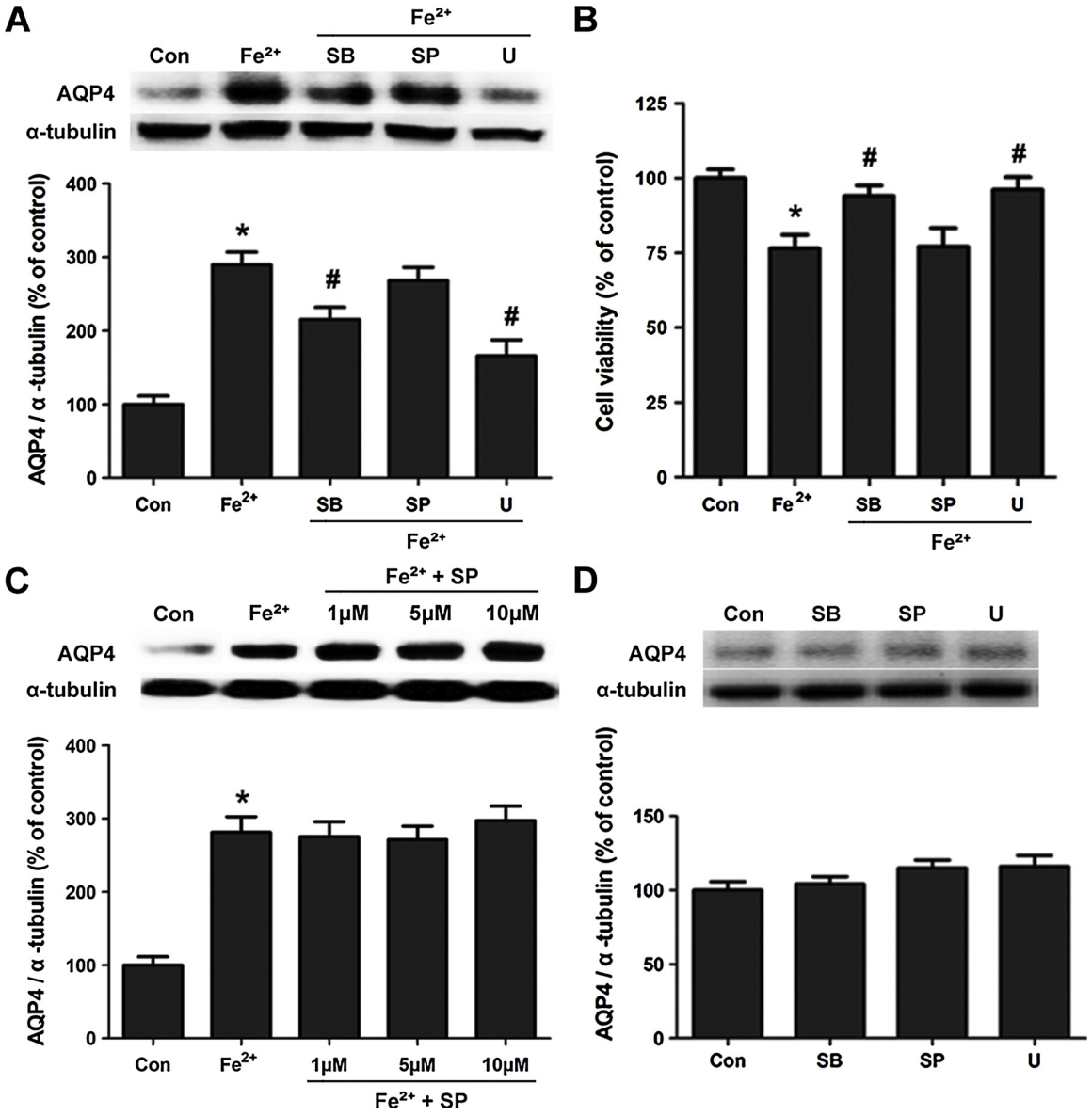

Fig. 6. Effect of MAPK inhibitors on Fe^{2+}-induced AQP4 upregulation and astrocyte death. (A, C and D) Both SB203580 (5 μM) and U0126 (5 μM) reduced AQP4 expression induced by Fe^{2+} significantly, while SP600125 (1–10 μM) did not inhibit the increased AQP4 expression. Treatment with MAPK inhibitors alone showed no significant influence on AQP4 protein expression. n = 3 for each group. Values are mean ± SE. *p < 0.05 vs. control group. #P < 0.05 vs. Fe^{2+}-exposure group. (B) Fe^{2+}-induced astrocyte death was attenuated by both SB203580 (5 μM) and U0126 (5 μM), but not by SP600125 (5 μM). n = 5 for each group. Values are mean ± SE. *p < 0.05 vs. control group. #P < 0.05 vs. Fe^{2+}-exposure group.

transcription of many genes associated with inflammation (Barnes and Karin, 1997). Activation of NF-κB is implicated in the increased expression of proinflammatory cytokines such as IL-1β, IL-6, IL-2, IL-10 and TNF-α (Laird et al., 2014; Malek et al., 2007; Ohnishi et al., 2014; Sigala et al., 2011; Wang et al., 2010; Yang et al., 2013a). Sun et al. demonstrated that incubation of cultured astrocytes with exogenous IL-6 could increase AQP4 expression, and this effect of IL-6 on AQP4 expression could be significantly reversed by the neutralizing anti-IL-6 antibody (Sun et al., 2017). These findings suggest that activation of NF-κB may regulate AQP4 expression through increased proinflammatory cytokines.

5. Conclusions

Fe^{2+} had distinctive toxic effects on cultured astrocytes, and increased AQP4 expression in cultured astrocytes. AQP4 gene silencing attenuated cell death after Fe^{2+} treatment, suggesting a key role of AQP4 in Fe^{2+}-induced astrocyte death. Inhibition of OS and MAPK signaling pathway reduced AQP4 expression in cultured astrocytes as well as cell death after Fe^{2+} overload, indicating the important role of OS and MAPK activation in Fe^{2+}-induced astrocyte death.

Conflict of interest

All authors certify that they have no affiliations with or involvement in any organization or entity with any financial interest.

Ethical approval

All applicable international, national, and/or institutional guidelines for the care and use of animals were followed. All procedures performed in studies involving animals were in accordance with the ethical standards of the institution or practice at which the studies were conducted.

Acknowledgements

This research was supported by a grant from the National Natural Science Foundation of China (81601054, 81671194, 81771318).

References

Adachi, T., Teramachi, M., Yasuda, H., Kamiya, T., Hara, H., 2012. Contribution of p38 MAPK, NF-kappaB and glucocorticoid signaling pathways to ER stress-induced increase in retinal endothelial permeability. Arch. Biochem. Biophys. 520, 30–35.

Arima, H., Yamamoto, N., Sobue, K., Umenishi, F., Tada, T., Katsuya, H., Asai, K., 2003. Hyperosmolar mannitol simulates expression of aquaporins 4 and 9 through a p38 mitogen-activated protein kinase-dependent pathway in rat astrocytes. J. Biol. Chem. 278, 44525–44534.

Barnes, P.J., Karin, M., 1997. Nuclear factor-kappaB: a pivotal transcription factor in chronic inflammatory diseases. N. Engl. J. Med. 336, 1066–1071.

Belaidi, A.A., Bush, A.I., 2016. Iron neurochemistry in Alzheimer's disease and Parkinson's disease: targets for therapeutics. J. Neurochem. 139 (Suppl. 1), 179–197.

Cassarino, D.S., Halvorsen, E.M., Swerdlow, R.H., Abramova, N.N., Parker Jr., W.D., Sturgill, T.W., Bennett Jr., J.P., 2000. Interaction among mitochondria, mitogen-activated protein kinases, and nuclear factor-kappaB in cellular models of Parkinson's disease. J. Neurochem. 74, 1384–1392.

Chi, Y., Fan, Y., He, L., Liu, W., Wen, X., Zhou, S., Wang, X., Zhang, C., Kong, H., Sonoda, L., Tripathi, P., Li, C.J., Yu, M.S., Su, C., Hu, G., 2011. Novel role of aquaporin-4 in CD4+ CD25+ T regulatory cell development and severity of Parkinson's disease. Aging Cell 10, 368–382.

Chu, H., Xiang, J., Wu, P., Su, J., Ding, H., Tang, Y., Dong, Q., 2014. The role of aquaporin 4 in apoptosis after intracerebral hemorrhage. J. Neuroinflammation 11, 184.

Crichton, R.R., Wilmet, S., Legssyer, R., Ward, R.J., 2002. Molecular and cellular mechanisms of iron homeostasis and toxicity in mammalian cells. J. Inorg. Biochem. 91, 9–18.

Dai, M.C., Zhong, Z.H., Sun, Y.H., Sun, Q.F., Wang, Y.T., Yang, G.Y., Bian, L.G., 2013. Curcumin protects against iron induced neurotoxicity in primary cortical neurons by attenuating necroptosis. Neurosci. Lett. 536, 41–46.

de Alvaro, C., Teruel, T., Hernandez, R., Lorenzo, M., 2004. Tumor necrosis factor alpha produces insulin resistance in skeletal muscle by activation of inhibitor kappaB kinase in a p38 MAPK-dependent manner. J. Biol. Chem. 279, 17070–17078.

Gunnarson, E., Axehult, G., Baturina, G., Zelenin, S., Zelenina, M., Aperia, A., 2005. Lead induces increased water permeability in astrocytes expressing aquaporin 4. Neuroscience 136, 105–114.

Higashida, T., Kreipke, C.W., Rafols, J.A., Peng, C., Schafer, S., Schafer, P., Ding, J.Y., Dornbos 3rd, D., Li, X., Guthikonda, M., Rossi, N.F., Ding, Y., 2011a. The role of hypoxia-inducible factor-1alpha, aquaporin-4, and matrix metalloproteinase-9 in blood-brain barrier disruption and brain edema after traumatic brain injury. J. Neurosurg. 114, 92–101.

Higashida, T., Peng, C., Li, J., Dornbos 3rd, D., Teng, K., Li, X., Kinni, H., Guthikonda, M., Ding, Y., 2011b. Hypoxia-inducible factor-1alpha contributes to brain edema after stroke by regulating aquaporins and glycerol distribution in brain. Curr. Neurovasc. Res. 8, 44–51.

Hua, Y., Nakamura, T., Keep, R.F., Wu, J., Schallert, T., Hoff, J.T., Xi, G., 2006. Long-term effects of experimental intracerebral hemorrhage: the role of iron. J. Neurosurg. 104, 305–312.

Hua, Y., Keep, R.F., Hoff, J.T., Xi, G., 2007. Brain injury after intracerebral hemorrhage: the role of thrombin and iron. Stroke 38, 759–762.

Huang, F.P., Xi, G., Keep, R.F., Hua, Y., Nemoianu, A., Hoff, J.T., 2002. Brain edema after experimental intracerebral hemorrhage: role of hemoglobin degradation products. J. Neurosurg. 96, 287–293.

Jiang, D., Li, X., Williams, R., Patel, S., Men, L., Wang, Y., Zhou, F., 2009. Ternary complexes of iron, amyloid-beta, and nitrilotriacetic acid: binding affinities, redox properties, and relevance to iron-induced oxidative stress in Alzheimer's disease. Biochemistry 48, 7939–7947.

Jung, J.S., Bhat, R.V., Preston, G.M., Guggino, W.B., Baraban, J.M., Agre, P., 1994. Molecular characterization of an aquaporin cDNA from brain: candidate osmoreceptor and regulator of water balance. Proc Natl Acad Sci U S A 91, 13052–13056.

Kyriakis, J.M., Avruch, J., 1996. Protein kinase cascades activated by stress and inflammatory cytokines. Bioessays 18, 567–577.

Laird, M.D., Shields, J.S., Sukumari-Ramesh, S., Kimbler, D.E., Fessler, R.D., Shakir, B., Youssef, P., Yanasak, N., Vender, J.R., Dhandapani, K.M., 2014. High mobility group box protein-1 promotes cerebral edema after traumatic brain injury via activation of toll-like receptor 4. Glia 62, 26–38.

Lane, D.J., Robinson, S.R., Czerwinska, H., Bishop, G.M., Lawen, A., 2010. Two routes of iron accumulation in astrocytes: ascorbate-dependent ferrous iron uptake via the divalent metal transporter (DMT1) plus an independent route for ferric iron. Biochem. J. 432, 123–132.

Lee, M., Lee, S.J., Choi, H.J., Jung, Y.W., Frokiaer, J., Nielsen, S., Kwon, T.H., 2008. Regulation of AQP4 protein expression in rat brain astrocytes: role of P2X7 receptor activation. Brain Res. 1195, 1–11.

Liu, L., Lu, Y., Kong, H., Li, L., Marshall, C., Xiao, M., Ding, J., Gao, J., Hu, G., 2012. Aquaporin-4 deficiency exacerbates brain oxidative damage and memory deficits induced by long-term ovarian hormone deprivation and D-galactose injection. Int. J. Neuropsychopharmacol. 15, 55–68.

Liu, B., Teschemacher, A.G., Kasparov, S., 2017. Astroglia as a cellular target for neuroprotection and treatment of neuro-psychiatric disorders. Glia 65, 1205–1226.

Malek, R., Borowicz, K.K., Jargiello, M., Czuczwar, S.J., 2007. Role of nuclear factor kappaB in the central nervous system. Pharmacol. Rep. 59, 25–33.

McCoy, E., Sontheimer, H., 2010. MAPK induces AQP1 expression in astrocytes following injury. Glia 58, 209–217.

Nico, B., Ribatti, D., 2011. Role of aquaporins in cell migration and edema formation in human brain tumors. Exp. Cell Res. 317, 2391–2396.

Ohnishi, M., Monda, A., Takemoto, R., Fujimoto, Y., Sugitani, M., Iwamura, T., Hiroyasu, T., Inoue, A., 2014. High-mobility group box 1 up-regulates aquaporin 4 expression via microglia-astrocyte interaction. Neurochem. Int. 75, 32–38.

Qian, Z.M., To, Y., Tang, P.L., Feng, Y.M., 1999. Transferrin receptors on the plasma membrane of cultured rat astrocytes. Exp. Brain Res. 129, 473–476.

Qing, W.G., Dong, Y.Q., Ping, T.Q., Lai, L.G., Fang, L.D., Min, H.W., Xia, L., Heng, P.Y., 2009. Brain edema after intracerebral hemorrhage in rats: the role of iron overload and aquaporin 4. J. Neurosurg. 110, 462–468.

Rao, K.V., Jayakumar, A.R., Reddy, P.V., Tong, X., Curtis, K.M., Norenberg, M.D., 2010. Aquaporin-4 in manganese-treated cultured astrocytes. Glia 58, 1490–1499.

Shenaq, M., Kassem, H., Peng, C., Schafer, S., Ding, J.Y., Fredrickson, V., Guthikonda, M., Kreipke, C.W., Rafols, J.A., Ding, Y., 2012. Neuronal damage and functional deficits are ameliorated by inhibition of aquaporin and HIF1alpha after traumatic brain injury (TBI). J. Neurol. Sci. 323, 134–140.

Shi, Z.M., Han, Y.W., Han, X.H., Zhang, K., Chang, Y.N., Hu, Z.M., Qi, H.X., Ting, C., Zhen, Z., Hong, W., 2016. Upstream regulators and downstream effectors of NF-kappaB in Alzheimer's disease. J. Neurol. Sci. 366, 127–134.

Sigala, I., Zacharatos, P., Toumpanakis, D., Michailidou, T., Noussia, O., Theocharis, S., Roussos, C., Papapetropoulos, A., Vassilakopoulos, T., 2011. MAPKs and NF-kappaB differentially regulate cytokine expression in the diaphragm in response to resistive breathing: the role of oxidative stress. Am. J. Physiol. Regul. Integr. Comp. Physiol. 300, R1152–1162.

Skjorringe, T., Burkhart, A., Johnsen, K.B., Moos, T., 2015. Divalent metal transporter 1 (DMT1) in the brain: implications for a role in iron transport at the blood-brain barrier, and neuronal and glial pathology. Front. Mol. Neurosci. 8, 19.

Song, T.T., Bi, Y.H., Gao, Y.Q., Huang, R., Hao, K., Xu, G., Tang, J.W., Ma, Z.Q., Kong, F.P., Coote, J.H., Chen, X.Q., Du, J.Z., 2016. Systemic pro-inflammatory response facilitates the development of cerebral edema during short hypoxia. J. Neuroinflamm. 13, 63.

Sun, L., Li, M., Ma, X., Feng, H., Song, J., Lv, C., He, Y., 2017. Inhibition of HMGB1 reduces rat spinal cord astrocytic swelling and AQP4 expression after oxygen-glucose deprivation and reoxygenation via TLR4 and NF-kappaB signaling in an IL-6-dependent manner. J. Neuroinflammation 14, 231.

Tang, Z., Sun, X., Huo, G., Xie, Y., Shi, Q., Chen, S., Wang, X., Liao, Z., 2013. Protective effects of erythropoietin on astrocytic swelling after oxygen-glucose deprivation and reoxygenation: mediation through AQP4 expression and MAPK pathway. Neuropharmacology 67, 8–15.

Wang, L., Zhang, X., Liu, L., Yang, R., Cui, L., Li, M., 2010. Atorvastatin protects rat brains against permanent focal ischemia and downregulates HMGB1, HMGB1 receptors (RAGE and TLR4), NF-kappaB expression. Neurosci. Lett. 471, 152–156.

Wang, B.F., Cui, Z.W., Zhong, Z.H., Sun, Y.H., Sun, Q.F., Yang, G.Y., Bian, L.G., 2015. Curcumin attenuates brain edema in mice with intracerebral hemorrhage through inhibition of AQP4 and AQP9 expression. Acta Pharmacol. Sin. 36, 939–948.

Wang, B., Li, W., Jin, H., Nie, X., Shen, H., Li, E., Wang, W., 2018a. Curcumin attenuates chronic intermittent hypoxia-induced brain injuries by inhibiting AQP4 and p38 MAPK pathway. Respir. Physiol. Neurobiol. 255, 50–57.

Wang, C., Yan, M., Jiang, H., Wang, Q., He, S., Chen, J., Wang, C., 2018b. Mechanism of aquaporin 4 (AQP 4) up-regulation in rat cerebral edema under hypobaric hypoxia and the preventative effect of puerarin. Life Sci. 193, 270–281.

Ward, R.J., Zucca, F.A., Duyn, J.H., Crichton, R.R., Zecca, L., 2014. The role of iron in brain ageing and neurodegenerative disorders. Lancet Neurol. 13, 1045–1060.

Wu, H., Zhang, Z., Li, Y., Zhao, R., Li, H., Song, Y., Qi, J., Wang, J., 2010. Time course of upregulation of inflammatory mediators in the hemorrhagic brain in rats: correlation with brain edema. Neurochem. Int. 57, 248–253.

Wu, H., Wu, T., Xu, X., Wang, J., Wang, J., 2011. Iron toxicity in mice with collagenase-induced intracerebral hemorrhage. J. Cereb. Blood Flow Metab. 31, 1243–1250.

Ximenes-da-Silva, A., 2016. Metal ion toxins and brain Aquaporin-4 expression: an overview. Front. Neurosci. 10, 233.

Yamamoto, M., Takeya, M., Ikeshima-Kataoka, H., Yasui, M., Kawasaki, Y., Shiraishi, M., Majima, E., Shiraishi, S., Uezono, Y., Sasaki, M., Eto, K., 2012. Increased expression of aquaporin-4 with methylmercury exposure in the brain of the common marmoset. J. Toxicol. Sci. 37, 749–763.

Yang, J., Liu, X., Zhou, Y., Wang, G., Gao, C., Su, Q., 2013a. Hyperbaric oxygen alleviates experimental (spinal cord) injury by downregulating HMGB1/NF-kappaB expression. Spine (Phila Pa 1976) 38, E1641–1648.

Yang, M., Gao, F., Liu, H., Yu, W.H., Zhuo, F., Qiu, G.P., Ran, J.H., Sun, S.Q., 2013b. Hyperosmotic induction of aquaporin expression in rat astrocytes through a different MAPK pathway. J. Cell. Biochem. 114, 111–119.

Yatsushige, H., Ostrowski, R.P., Tsubokawa, T., Colohan, A., Zhang, J.H., 2007. Role of c-Jun N-terminal kinase in early brain injury after subarachnoid hemorrhage. J. Neurosci. Res. 85, 1436–1448.

Yuen, C.M., Yeh, K.H., Wallace, C.G., Chen, K.H., Lin, H.S., Sung, P.H., Chai, H.T., Chen, Y.L., Sun, C.K., Chen, C.H., Kao, G.S., Ko, S.F., Yip, H.K., 2017. EPO-cyclosporine combination therapy reduced brain infarct area in rat after acute ischemic stroke: role of innate immune-inflammatory response, micro-RNAs and MAPK family signaling pathway. Am. J. Transl. Res. 9, 1651–1666.

Yukutake, Y., Tsuji, S., Hirano, Y., Adachi, T., Takahashi, T., Fujihara, K., Agre, P., Yasui, M., Suematsu, M., 2008. Mercury chloride decreases the water permeability of aquaporin-4-reconstituted proteoliposomes. Biol. Cell 100, 355–363.